J Comp Physiol A (2001) 187: 131–144
DOI 10.1007/s003590100183

ORIGINAL PAPER

Volker Dürr · Yvonne König · Rolf Kittmann

The antennal motor system of the stick insect *Carausius morosus*: anatomy and antennal movement pattern during walking

Accepted: 8 January 2001 / Published online: 22 February 2001

Abstract The stick insect *Carausius morosus* continuously moves its antennae during locomotion. Active antennal movements may reflect employment of antennae as tactile probes. Therefore, this study treats two basic aspects of the antennal motor system: First, the anatomy of antennal joints, muscles, nerves and motoneurons is described and discussed in comparison with other species. Second, the typical movement pattern of the antennae is analysed, and its spatio-temporal coordination with leg movements described. Each antenna is moved by two single-axis hinge joints. The proximal head-scape joint is controlled by two levator muscles and a three-partite depressor muscle. The distal scape-pedicel joint is controlled by an antagonistic abductor/adductor pair. Three nerves innervate the antennal musculature, containing axons of 14–17 motoneurons, including one common inhibitor. During walking, the pattern of antennal movement is rhythmic and spatio-temporally coupled with leg movements. The antennal abduction/adduction cycle leads the protraction/retraction cycle of the ipsilateral front leg with a stable phase shift. During one abduction/adduction cycle there are typically two levation/depression cycles, however, with less strict temporal coupling than the horizontal component. Predictions of antennal contacts with square obstacles to occur before leg contacts match behavioural performance, indicating a potential role of active antennal movements in obstacle detection.

V. Dürr (✉)
Abteilung für Biologische Kybernetik
und Theoretische Biologie, Fakultät für Biologie,
Universität Bielefeld,
Postfach 10 01 31, 33501 Bielefeld, Germany
E-mail: volker.duerr@biologie.uni-bielefeld.de
Fax: +49-521-1062963

Y. König · R. Kittmann
Institut für Biologie I (Zoologie), Fakultät für Biologie,
Universität Freiburg, Hauptstraße 1,
79104 Freiburg, Germany

Key words Antennal movement · Tactile sense · Antennal muscle · Motoneuron · Limb coordination

Abbreviations *Ab1–4* abductor motoneuron 1–4 · *Ad1–3* adductor motoneuron 1–3 · *AEP*: anterior extreme position · *AL* antennal lobe · *AMMC* antennal mechanosensory and motor complex · *aTB* anterior tentorial branch · *cMD* central part of MD · *CI* common inhibitor · *CT* corpus tentorium · *Dp1–5* depressor motoneuron 1–5 · *dTB* dorsal tentorial branch · *lMD* lateral part of MD · *lML* lateral levator muscle · *Lv1–4* levator motoneuron 1–4 · *MD* depressor muscle · *mMD* medial part of MD · *mML* medial levator muscle · *N1–4* antennal nerves 1–4 · *PEP* posterior extreme position · *pTB* posterior tentorial branch · *Tn2/3* tract of N2 and N3 · *Tn4* tract of N4

Introduction

Stick insects of the species *Carausius morosus* vigorously move their antennae during walking. Because the antennae are of the same length as the front legs, antennal contacts always signal the presence of an object within the action range of the front legs. Antennal contacts therefore provide tactile information that could be exploited by the animal to adapt its on-going locomotor pattern to the spatial conditions immediately ahead. The aim of the current study is to establish a basis for understanding the tactile use of the stick insect antennae. This includes an anatomical description of antennal joints, muscles, nerves and motoneurons, but also a functional analysis of the typical antennal movement pattern during walking.

Among all insect senses, the tactile sense is probably the least studied. Judging from our knowledge about insect vision (Stavenga and Hardie 1989), hearing (Hoy et al. 1998), olfaction (Hansson 1999) or proprioception (Mill 1976; Field and Matheson 1998), one may wonder whether any insect would need further sensory infor-

mation to survive. In case of information about space, processing of tactile cues can be expected to be both faster and less costly than processing of visual cues, because the geometry of the own body is inherently known and can be used to immediately interpret external object locations in a body coordinate framework. Furthermore, for nocturnal insects or species that live in environments with poor light conditions, vision may not be of much help at all.

In walking insects – and many insect species spend a great deal of their life walking about – information about the spatial arrangement of the immediate surroundings of the animal can be expected to be beneficial, for example, to quickly adapt the locomotor pattern to forthcoming obstacles. The antennae, or feelers, of the stick insect must be considered a major source of tactile information, firstly because they carry mechanoreceptors (Cappe de Baillon 1936; Weide 1960; Slifer 1966) and secondly because stick insects constantly move their antennae during locomotion and thereby raise the probability of antennal contacts with obstacles. The use of antennae as tactile probes in other insect species has been demonstrated by discrimination and learning studies on honeybees (Kevan and Lane 1985; Erber et al. 1997, 1998). So far, the use of antennal tactile cues in locomotion has been demonstrated only for body axis adjustment in beetles (Schneider and Reitberger 1988; Pelletier and McLeod 1994).

The stick insect *C. morosus* is a model organism for locomotion studies (e.g. Bässler 1983; Cruse 1990) and its walking behaviour can be modelled in good approximation to real life (Cruse et al. 1998). However, current understanding of stick insect locomotion is restricted to the thorax and legs, neglecting the possible benefits of actively moved antennae. Despite the fact that active antennal movement is obvious to any observer, nothing is known about the movement pattern, how it comes about and whether it is connected to the stepping pattern of the legs. Moreover, the potential use of antennal tactile cues in motor behaviour has never been dealt with in this species. The present study is a prerequisite for understanding antennal tactile function in the stick insect, as it deals with two basic aspects of the antennal motor system: (1) the anatomy of antennal muscles and their innervation, and (2) the spatio-temporal pattern of antennal movement during locomotion.

Comparative anatomy of the antennal motor system will be discussed for the cricket *Gryllus campestris* (Honegger et al. 1990), the locust *Locusta migratoria* (Gewecke 1972; Bauer and Gewecke 1991), the tobacco moth *Manduca sexta* (Kloppenburg et al. 1997) and the honeybee *Apis mellifera* (Snodgrass 1956; Kloppenburg 1995).

Preliminary accounts of parts of this study have been published in abstract form (Kittmann and König 1995; Dürr 1999).

Materials and methods

All experiments were carried out on adult female stick insects of the species *C. morosus* Brunner 1907. Animals were taken from parthenogenetic laboratory cultures in Freiburg (anatomy) or Bielefeld (behaviour). Intactness of antennae was assessed by their length, which is approximately equal to that of the front legs.

Anatomy of antennal muscles and nerves

To study the anatomy of antennal muscles, animal heads were dissected under a stereo lens and dorsal, lateral or medial preparations were video-recorded. The spatial arrangement and insertions of the five antennal muscles could be worked out by sequential removal of all muscles. Single frames of the video tape were then traced for schematic drawings (Fig. 1). For comparison, a series of frontal sections through the entire head was made from a freshly moulted animal. The animal was decapitated and its head fixated in AAF for a few weeks, then embedded in paraffin, cut into 10-μm sections and stained with Bouin's dye (for details see Romeis 1989).

In order to trace the innervation of the antennal musculature in a macroscopic preparation, the nervous tissue was stained in situ, by use of a 0.02% Janus-Green B solution (Fluka) according to Yack (1993) in physiological Ringer-saline (Weidler and Diecke 1969). After 5–60 s of incubation, the dye was washed out with Ringer saline.

Neuroanatomy

For retrograde staining of antennal nerves, a heavy-metal impregnation was applied (Altman and Tyrer 1980). Either 1.5–5% $CoCl_2$ (Aldrich), hexamine-$CoCl_2$ (Fluka) or $NiCl_2$ solutions (Sigma) were used. Heavy-metal salts were precipitated by application of either ammonium sulphide (Aldrich) or rubeanic acid di-thio-oxamide (Merck, according to Quicke and Brace 1979) and fixated either with Carnoy's solution (Strausfeld and Miller 1980) or, in case of rubeanic acid precipitation, in neutral, buffered formaline (Romeis 1989). Finally, the preparation was dehydrated in a 50–100% ethanol chain and cleared in salicylic acid methyl ester.

To make individual nerve stumps accessible for backfills, the entire animal brain was isolated from the head capsule by means of a dorsal preparation: First the dorsal head cuticle and fat sheath were removed, then both optic lobes, the suboesophageal connectives, the Labrum nerves and the antennal nerves were severed, the latter distally to the scape. The isolated cerebral ganglion was placed in a Petri dish coated with silicon gum. The nerve stump to-be-dyed was stuck into a liquid-tight chamber made from Vaseline, and soaked in aqua dest. for approx. 5 min. in order to improve dye uptake. The water was then replaced by the dye solution and the dying-chamber was covered by a Vaseline lid. Finally, the Petri dish was filled with Ringer solution and kept at 4°C for 8–10 h.

For spatially focused staining of the antennal motor efferences, a vital-staining technique according to Bräunig (1985) was applied, where heavy-metal ions were iontophoretically injected straight into the deutocerebrum. Animals were immobilised and the head capsule was opened dorsally. A wide-tip glass microelectrode containing the dye solution was placed close to the region of the antennal mechanosensory and motor centre (AMMC) and a reference electrode was placed in the abdomen. Dye was then injected over a period of 2 h with pulsed current injections at a frequency of 1 Hz, 500 ms pulse duration and 10–50 μA. After injection, the dye was left to diffuse for 6–8 h at 4°C. To avoid desiccation of the brain, the wound was sealed with Vaseline. Subsequent processing of the preparation was the same as described for retrograde staining. Additionally, to enhance visibility of fine neuronal structures, Timms silver intensivation was applied, following Obermayer and Strausfeld (1980).

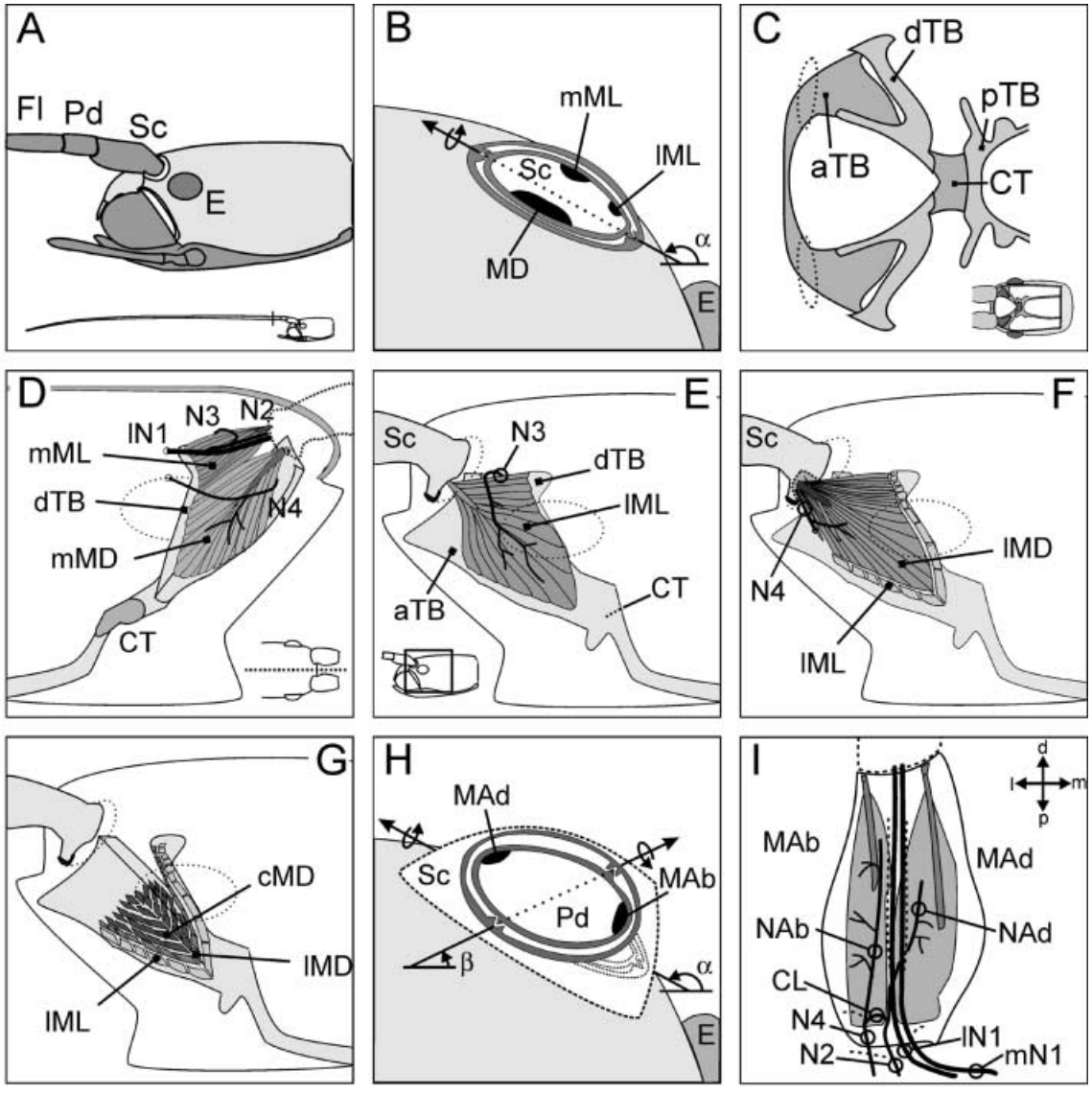

Fig. 1A–I Segments, muscles and joints of the stick insect antennae. Semi-schematic drawings of the head (**A**), the head-scape-joint (**B**) with its muscles and their insertions (**C–G**) and the scape-pedicel-joint with its muscles (**H, I**) of the stick insect. **A** Side view of the head, displaying insertion site of the left antenna relative to the eye (*E*) and mouth parts. The antenna has three functional segments: the scape (*Sc*) pedicel (*Pd*) and flagellum (*Fl*, clipped). The full length of the Fl is indicated by the inset. **B** Frontal view of the left antennal base. Angulation points of the head-scape-joint and distal insertion sites of the two levator muscles, lateral levator muscle (*lML*) and medial levator muscle (*mML*), and the three parts of the depressor muscle (*MD*). The rotation axis of this joint with its angle to the horizontal plane ($\alpha = 149°$) is indicated by the *arrow*. The left eye (*E*) is drawn for reference. **C** Dorsal view of the tentorium that serves as the proximal insertion site of the three muscles that move the scape. It consists of the central corpus tentorium (*CT*) and bilaterally symmetric anterior, dorsal and posterior tentorium branches (*aTB*, *dTB* and *pTB*, respectively). The pTB is clipped. The location of the tentorium inside the head is indicated by the inset. **D** Sagittal section through the head (*see inset*) with medial view of the medial levator muscle (*mML*) and the medial part of the depressor muscle (*mMD*). Proximal parts of the antennal motor nerves N2–N4 and of main antennal nerve N1 are shown. Locations of the scape and the eye are indicated by *dotted lines*. **E** Lateral view of the lML after cutting a window into the left side of the head (*see inset*), with distal branch of N3. Locations of the antennal ring and the eye are indicated by *dotted lines*. **F** Same view as in **E**, after removal of the lML, revealing its V-shaped basal insertion site along aTB and dTB. The lateral part of the depressor muscle (*lMD*) and its innervating branch of N4 are visible. **G** Same view as in **E** and **F**, after removal of all muscles. The proximal insertion sites of lML, lMD are V-shaped and juxtaposed to the triangular insertion area of the central part of the depressor muscle (*cMD*). **H** Frontal view of the left antenna cut at the base of the pedicel. Angulation points of the scape-pedicel-joint and the distal insertion sites of the abductor and adductor muscles are shown. *Black arrows* indicate rotation axes of the antennal joints. The widest cross-section of the scape and the location of the head-scape-joint (as in **B**) are depicted by *dotted lines*. Angles of the rotation axis of the head-scape-joint ($\alpha = 149°$), of the scape-pedicel-joint ($\beta = 28°$) are indicated. **I** Dorsal view of the left scape, after removing the dorsal surface (*arrows* indicate lateral-medial, distal-proximal). The laterally located abductor muscle (*MAb*) and medially located adductor muscle (*MAd*) insert on the base of the pedicel via long apodemes (*dark*). MAb and MAd are innervated by the abductor nerve (*NAb*) and the adductor nerve (*NAd*), respectively. NAb and NAd both contain fibres from each of the antennal nerves N2 and N4, which are connected by a cross-link (*CL*). The lateral, lN1, and medial, mN1, branch of the main antennal nerve traverse the scape. Sensory nerve branches are indicated by dotted lines at the base of the scape. Scales: box width is approximately 8 mm in **A** (inset ca. 36 mm), 1.5 mm in **B** and **H**, 2.5 mm in **C**, 3.2 mm in **D–G** and 2 mm in **I**

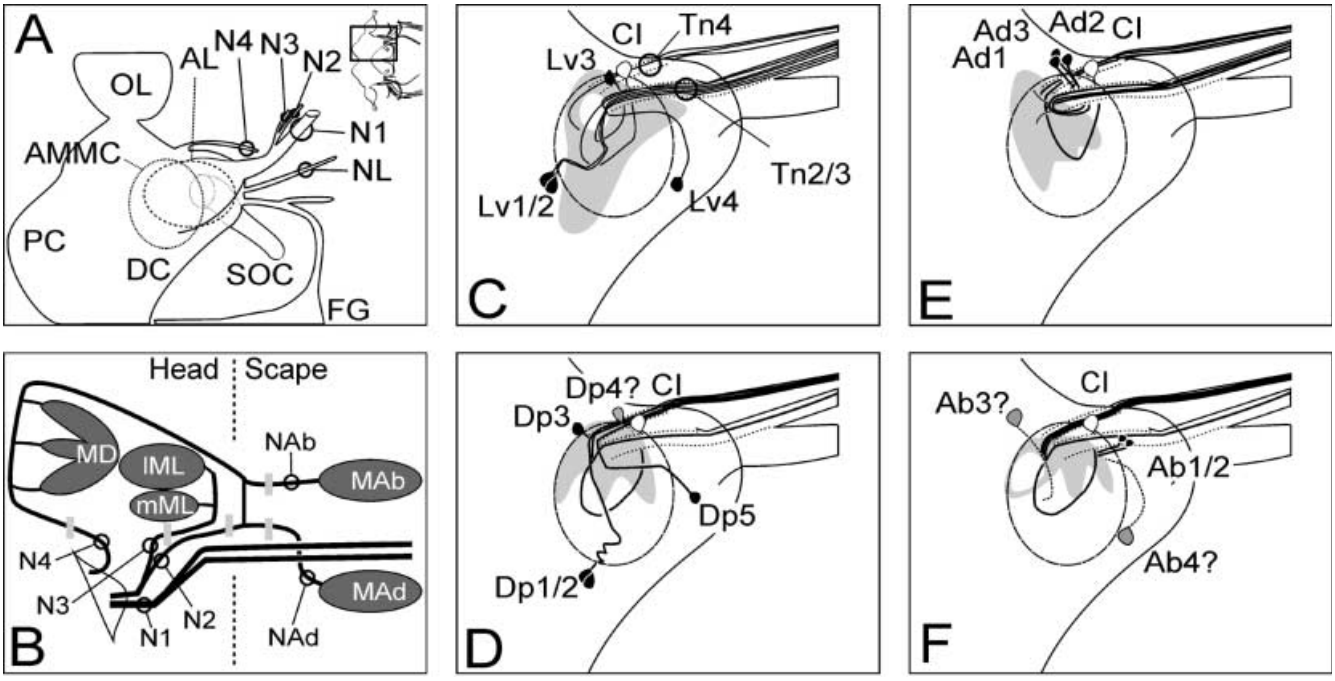

Fig. 2A–F Antennal nerves and motoneurons. **A** Semi-schematic dorsal view of the left half of the brain (*see inset*), showing the locations of the antennal lobe (*AL*, *dashed oval*) and the antennal mechanosensory and motor centre (*AMMC*, *dotted oval*), as well as the roots of the four antennal nerves (N1-4) and the labrum nerve (*NL*). *DC* deutocerebrum; *FG* frontal ganglion; *OL* optic lobes; *PC* protocerebrum; *SOC* suboesophageal connective. **B** Schematic innervation diagram of the antennal muscles (*MD*, depressor complex; *LML*, lateral levator; *mML*, medial levator; *MAb*, abductor; *MAd*, adductor) by the four antennal nerves (N1–N4). *Grey bars* mark the cut locations for backfills. The *vertical dotted line* indicates the location of the head-scape-joint. *NAd*, adductor nerve; *NAb*, abductor nerve. **C–F** Somata and main neurites of five levator motoneurons (**C** Lv1–Lv4 and common inhibitor, *CI*), six depressor motoneurons (**D** Dp1–Dp5 and CI), four adductor neurons (**E** Ad1–Ad3 and CI) and five abductor motoneurons (**F** Ab1–Ab4 and CI). *White soma* in each diagram depicts the CI. *Question marks and dark grey somata* label putative motoneurons with uncertain course of the main neurite. *Grey areas* delimit the approximate area of dendritic arborisation of motoneurons in the AMMC (*dashed oval*). The two motoneuron tracts Tn2/3 and Tn4 are indicated by *dotted lines* and labelled in **C**. Scales: length of boxes is approximately 2.5 mm in **A** and 0.9 mm in **C–F**. Orientation in all panels: rostral to the right; lateral to the top

Behavioural observations

Antennal and leg movements were studied in freely walking animals on a 40-mm-wide bridge of 400 mm length. In order to minimise visual input, the immediate environment was kept in black and the set-up was illuminated by an infrared spotlight. Animals were video-recorded from above and simultaneously, via a mirror, from the side. The video system consisted of a CCD-camera (Fricke, CCD-7250, 1-ms shutter, 50 Hz), a frame code generator (Magnasonic, VTG 200) and an sVHS video recorder (Blaupunkt RTV-925 or similar). Filming distance was 900 mm, and spatial resolution was 0.32 mm per pixel. For spatial analysis, video sequences were captured as non-compressed AVI-files (Microsoft video format) to an IBM-compatible computer via the graphics card (Elsa Victory Erazor), and manually digitised by use of a custom-written program (Borland Delphi). Digitising error, as estimated from repeated analysis of the same sequence, was less than 1 mm. In each frame, the position of both front-leg coxae and tibia-tarsus-joints, the antennal end-points and the body axis were determined for both the top view and the side view (mirror image) of the animal. The body axis was defined as the line from between the hind leg coxae to the distal point on the head, lying between the head-scape-joints. The latter point was also used as the proximal end of both antennae, and the reference point for the polar plots in Fig. 4. Given an antennal length of 30 mm and an antennal base distance of ca. 1.8 mm, this simplification resulted in a horizontal error angle of less than 1.75°, which is small compared to the observed movement angles. Further possible error sources were introduced by small head movements and by the curvature of the antennae. Both of these effects will be addressed specifically in the results section (Figs. 3, 4).

Results

General morphology

Like all pterygote insect antennae (Imms 1939), the antennae of the stick insect possess three functional segments, the two short basal segments scape and pedicel, and a long thin flagellum (Fig. 1A). Active movements of the antenna are restricted to the joint between the head capsule and the scape, and the joint between the scape and the pedicel. The flagellum, on which the majority of sensory hairs are located, contains no muscles and can therefore be moved or bent only passively. Morphologically, the flagellum is constituted by several segments, the shape and sensory repertoire of which changes gradually along its length (Weide 1960; Slifer 1966). Because the flagellum can be viewed as a passively moved multisensory probe, which is not part of the active antennal motor apparatus, it will not be considered any further in this study.

Because the antennae of the insect orders Phasmatodea (stick and leaf insects) and Ensifera (crickets

and grasshoppers) bear many similarities, most of which are likely homologies, the terminology for muscles, nerves and motoneurons is largely adapted to the work of Honegger et al. (1990) on the cricket.

The head-scape joint

The scape is the most proximal antennal segment. It connects to the head capsule via a soft joint membrane, which is narrowed ventro-laterally and dorso-medially, where the sclerotised cuticle forms two condyli. The line between these two condyli defines the axis of rotation of this hinge joint (Fig. 1B). As the lateral condylus is located anterior-ventrally with respect to the medial condylus, the axis of rotation is tilted $10 \pm 3°$ medially with respect to the frontal plane and $149 \pm 7°$ dorsally with respect to the horizontal plane ($n = 8$ animals; values are mean $\pm$ SD).

Active movement of the scape is achieved by contraction of a set of three muscles, which originate from the tentorium, an internal cuticular structure (Fig. 1C), and distally insert at the base of the scape (Fig. 1B). Because these tentorio-scapal muscles completely lie outside the antenna, i.e. inside the head capsule, they have been called 'extrinsic' antennal muscles by Imms (1939). In the stick insect, tentorio-scapal muscles can be functionally divided into a pair of levator muscles, contractions of which move the antenna dorso-laterally, and a depressor muscle, contractions of which move the antenna ventro-medially.

On its proximal end, the medial levator muscle (mML), inserts on the dorsal tentorium branch (dTB) (Fig. 1D), along which it attaches to the dorsal part of the medial surface. The lateral levator muscle (lML) (Fig. 1E) is the most lateral muscle of the antennal motor system. Its proximal insertion site is V-shaped, with one shank of the V running along the anterior tentorium branch (aTB), and the other shank along the lateral surface of the dTB (Fig. 1E, F). It is a large muscle covering the lateral and central part of the depressor muscle. The depressor muscle proximally splits into three parts. The lateral part of the depressor (lMD), becomes visible only after removal of the lML (Fig. 1F). Its proximal insertion is also V-shaped, and juxtaposed to that of the lML (Fig. 1G). The central part of the depressor (cMD) is located underneath the lMD and inserts on the remaining dorsal surface of the aTB (Fig. 1G). The third, medial part of the depressor muscle, mMD, inserts below the medial levator on the medial surface of the dTB as well as on the medial edge of the aTB (Fig. 1D). The three parts of the depressor muscle have a common distal insertion site on the ventro-medial rim of the scape (Fig. 1B). The two levator muscles have separate distal insertion sites. The mML

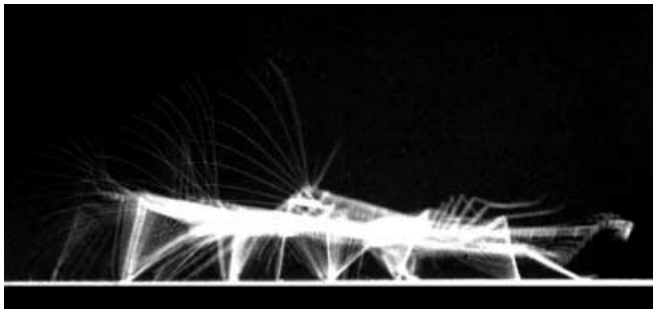

Fig. 3 *Carausius morosus* vigorously moves its antennae during walking. Photograph of a walking stick insect under 50-Hz stroboscopic illumination. Exposure time was 1 s, approximately equalling the time for a single step cycle of each leg. Walking direction is from right to left. The left antenna is moved down and up twice. The right antenna can be seen only faintly, as it is mostly out of focus. Note that the shape of the left antenna remains almost unchanged even during the fast antennal movements

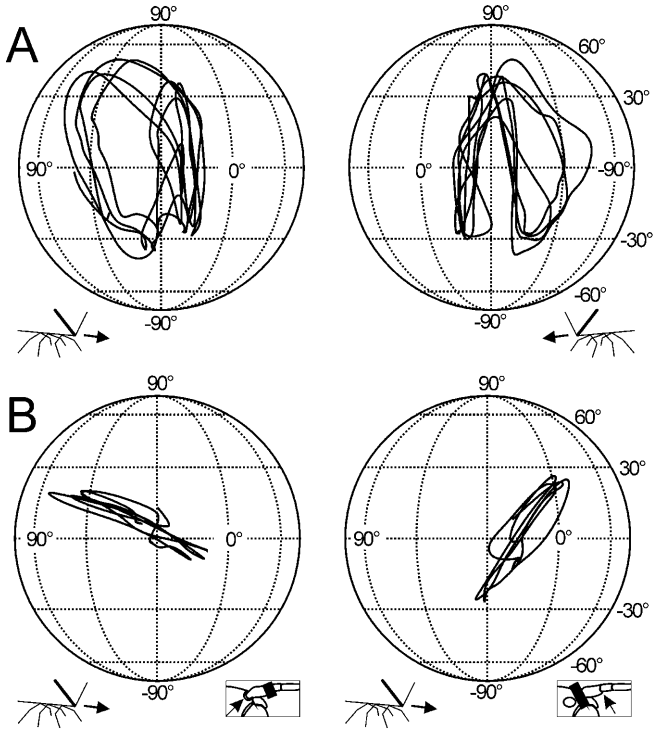

Fig. 4A, B The typical antennal movement pattern during walking and degrees of freedom of antennal movements. **A** Typical movement pattern of right and left antennae during walking (*left sphere*: right antenna; *right sphere*: left antenna). Trajectories of antennal tips are shown as polar coordinates in a sphere, the centre of which corresponds to the base of the antenna. *Horizontal lines* mark elevation and elliptic lines mark the azimuth. The body axis points towards the 0° label (*see inset stick drawings*). The spheres are rotated 30° medially to show the ipsilateral frontal sector of each antenna. The illustrated trajectories lasted 5 s and correspond to five subsequent step cycles of all legs. **B** Trajectories of antennal movement with one of the two antennal joints fixed. *Left*: movement restricted to head-scape joint; scape-pedicel-joint fixed. *Right*: head-scape joint fixed; movement restricted to scape-pedicel-joint (*see insets below*). The two graphs illustrate coincident trajectories of both antennae during a 2-s walking episode of a single animal. Trajectory of left antenna was illustrated mirror-symmetrically, in order to allow direct comparison of joint action rages. Same graph details as above

attaches to the dorsal rim of the scape, whereas the lML attaches more laterally (Fig. 1B).

The scape-pedicel-joint

The pedicel is the second antennal segment. It is approximately cylindrical in shape and about half the length of the scape. Like the head-scape-joint, the scape-pedicel-joint is a hinge joint with two cuticular condyli (Fig. 1H) and a soft joint membrane. The centre of a proximal pedicel cross-section is shifted medially relative to the base of the scape, lying approximately in front of the medial head-scape condylus. As the lateral condylus is located more dorsally than the medial condylus the scape pedicel-axis is rotated $28 \pm 8°$ dorsally with respect to the horizontal plane ($n = 8$ animals). As a consequence, the projections of the two joint axes are neither parallel in the horizontal plane (top view), nor perpendicular in the frontal plane. In a frontal view, they form an angle of $59 \pm 3°$ between each other (Fig. 1H).

The pedicel can be moved by a pair of antagonistic scapo-pedicellar muscles (Fig. 1I). These muscles are located entirely inside the scape, and therefore have been called 'intrinsic' antennal muscles by Imms (1939). The lateral scapo-pedicellar muscle distally inserts on the lateral rim of the pedicel and therefore moves the antenna ventro-laterally. Here, it is termed the antennal abductor (MAb in Fig. 1H, I). Its antagonist, the medial scapo-pedicellar muscle, distally inserts at the dorso-medial rim of the pedicel, moving the antenna dorso-medially, making it the antennal adductor (MAd in Fig. 1H, I). Both scapo-pedicellar muscles act via long apodemes.

Antennal nerves

Four antennal nerves leave the deutocerebrum (Fig. 2A). The main antennal nerve (N1) is an exclusively sensory nerve. Proximal to the level of the head-scape-joint, the N1 divides into a lateral (lN1) and a medial branch (mN1) (Fig. 2B). Both branches traverse the centre of the scape (Fig. 1I) and proceed through the pedicel and the entire flagellum, where they innervate all sensory hairs. Inside the scape, both lN1 and mN1 give off smaller branches which innervate various sensory receptors on the scape and pedicel (not shown).

Antennal nerves N2 and N3 leave the deutocerebrum in a common sheath together with N1, which they part at the level of the mML (Fig. 1D). N2 runs in parallel to N1 until the head-scape joint, where it gives off a lateral sensory side branch, innervating mechanoreceptors in the vicinity of the head-scape joint. Antennal nerve N3 runs on the medial surface of mML where it innervates this muscle by side branches. It then traverses the dorsal margin of mML and lML and descends to innervate both the mML and the lML on their lateral surface (Fig. 1D, E). It is therefore the levator nerve.

The fourth nerve, N4, leaves the deutocerebrum separately from the other antennal nerves (Fig. 2A, B), runs round the frontal margin of the lMD and innervates it on its antero-lateral surface (Fig. 1F). Another branch of N4 innervates the mMD. A large branch of N4 ascends into the scape where it forms a cross-connection with N2 (Figs. 1I, 2B). Because in this link fibres of both nerves cross sides, the nerves distal to it are composed of different sets of neurons. They therefore are re-named the 'adductor nerve' (NAd) continuing on the medial side in continuation of N2, and a lateral 'abductor nerve' (NAbd) the continuation of N4 (Figs. 1I, 2B). According to their names, the NAd and NAb innervate the medially located adductor muscle and the laterally located abductor muscle, respectively. The NAb also gives off a sensory side branch, innervating mechanoreceptors at the base of the scape.

Note that the anatomical situation is subject to considerable variability. The descriptions given above are representative in that they describe the most common situation.

Motoneurons

Based on the anatomical descriptions of the previous section, it was possible to determine five locations for nerve backfills, which would allow a correct functional assignment of each dyed motoneuron to a given muscle or set of muscles. These locations are indicated in Fig. 2B. A total of 80 backfills were made. Each of the described motoneurons was found in at least three specific nerve backfills. According to the branching pattern of the antennal nerves, the motoneuron axons enter the brain via two tracts: axons from N4 form a separate tract (Tn4) from the axons in the other two motor nerves, which enter via the Tn2/3 (Fig. 2C).

The four functional groups of motoneurons, i.e. levator, depressor, adductor and abductor motoneurons, are shown in Fig. 2C–F, respectively. Motoneurons of the same functional group were numbered according to the location of their somata: clockwise from postero-medial to antero-medial. The somata of all motoneurons are located in the deutocerebrum, in the periphery of the antennal lobe,(AL) and the so-called AMMC (Rospars 1988; Homberg et al. 1989). In *Carausius morosus* the AL is restricted to the dorsal part of the deutocerebrum, whereas the AMMC is located ventrally and slightly more posterior. Each motoneuron soma can be assigned to one of three locations: (1) a region posterior to the AL and posterio-dorsal to the AMMC, (2) a region antero-dorsally of the AMMC, and (3) a lateral region close to the roots of the antennal nerves. Table 1 lists the soma locations of all motoneurons with respect to these three soma regions.

A detailed description of the dendritic arborisations of the stained motoneurons is beyond the scope of this study, because complete stains of all dendrites were not obtained for all motoneurons. Nevertheless, the ap-

Table 1 Total number and locations of motoneuron somata according to functional groups and soma regions (*Ab1–Ab4* abductor motoneurons 1–4, *Ad1–Ad3* adductor motoneurons 1–3, *CI* common inhibitor, *Dp1–Dp5* depressor motoneurons 1–5, *Lv1–Lv4* levator motoneurons 1–4, *Lv1/2* and *Dp1/2* are twin neurons, *?* rare or incomplete stains)

	Total	Posterior	Lateral	Anterior
Levator	4 + CI	Lv1/2	Lv3 and CI	Lv4
Depressor	4–5 + CI	Dp1/2	Dp3?, Dp4 and CI	Dp5
Adductor	3 + CI	–	Ad1–3 and CI	–
Abductor	2–4 + CI	–	Ab1–2, Ab3? and CI	Ab4?

proximate area of dendritic arborisation is indicated for each functional group (grey shaded area in Fig. 2C–F). Good stains often revealed twins of neurons with parallel neurites and perfectly overlapping dendritic fields.

Common inhibitor

One particular soma of the lateral soma region was found in preparations from all antennal motor nerves, indicating that this neuron innervates all antennal muscles. Its neurite forms a characteristic loop through the AMMC, then bifurcates and enters both tract Tn4 and tract Tn2/3. As these features have been commonly described for inhibitory motoneurons of insect motor systems, it was termed the common inhibitor, CI (white soma in Fig. 2C–F). The Tn2/3 branch crosses the N2/N4-crosslink such that NAb-backfills labelled an axon in tract Tn2/3 which continued distally in both N2 and N3, whereas NAd- and distal N3-backfills also stained an axon in N4, innervating the depressor. The CI-innervation of the MAb is variable between animals and may be a continuation of N4 or of N2.

Levator motoneurons

N3-backfills revealed five neurons innervating lML and mML (Lv1–4 and CI, Fig. 2C). The axons of all levator motoneurons leave the deutocerebrum via tract Tn2/3. In some preparations, only one neuron of the pair Lv1/2 was stained. In some occasions, a second soma was found in the vicinity of Lv4 with a similar neurite as Lv4. The area of dendritic arborisation of levator motoneurons is restricted to the antero-lateral and the postero-medial to postero-lateral part of the AMMC. A circular patch without dyed dendrites was frequently observed in the postero-lateral part of the AMMC.

Depressor motoneurons

Proximal N4-backfills and their comparison with NAb- and NAd-backfills revealed 6 depressor motoneurons (Dp1–5 and CI, Fig. 2D). All but the CI have their axon exclusively in tract Tn4. The soma of neuron Dp4 was visible only in a few stains and its neurite couldn't be reliably traced. Also, since the NAb-backfills were somewhat unreliable due to the relatively long diffusion distance, there is a chance of misinterpreting abductor motoneurons as depressor motoneurons. The area of dendritic arborisation of Dp1–5 is restricted to the lateral part of the AMMC.

Adductor motoneurons

NAd-backfills result in the staining of four motoneurons (Ad1–3 and CI, Fig. 2E). The axons of Ad1 and Ad2 cross tract Tn2/3 and then turn in a characteristic loop into tract Tn2/3, from where they ascend through N2 into NAd. The axon of Ad3 follows the same turn as Ad1–2 but then enters the Tn4, ascends through N4 and finally crosses over to the N2 branch to join the NAd. The area of dendritic arborisation of adductor motoneurons extends from the posterio-lateral AMMC into its centre.

Abductor motoneurons

The abductor muscle is innervated by at least three, probably five motoneurons (Ab1–4 and CI, Fig. 2F). The neurons Ab1 and Ab2 enter tract Tn4 to ascend through N4. While the somata of two further putative abductor motoneurons were clearly dyed (Ab3 and Ab4), their axons could not be traced reliably and may use the N4 or the N2 pathway. The abductor motoneurons show an area of dendritic arborisation similar to that of the depressor motoneurons, but sparing a posterior patch in the AMMC.

In some cases of N2-backfills or multiple backfills of several nerves, 1–3 protocerebral somata were stained. Their axons run medially, ventral to the AMMC and ascend to the posterior protocerebrum, where their somata are located medial to the mushroom bodies.

Antennal movements

Typical pattern during walking and degrees of freedom

During walking, *C. morosus* vigorously moves its antennae (Fig. 3). Much like the rhythmic leg-movements, the antennae are also moved with a characteristic rhythmic pattern. A closer look at the photography in Fig. 3 reveals that the shape of the flagellum hardly changes during the fast up-and-down movements. Therefore, the stiffness of the flagellum is sufficient to maintain the typical shape during fast antennal movements. Nevertheless, the flagellum can be bent passively, e.g. due to contact with objects. The typical shape of the antennae exhibits a slight ventral curvature in the distal third of the flagellum, such that the tip of the antenna is located approximately 8° more ventral than the direction

of the flagellar base would suggest. If the mass of the antennal tip was large enough for gravity to cause the distal curvature of the flagellum, then its inertia should cause an upward flexion during fast downstrokes of the flagellum. This was not observed. Accordingly, we assume a morphological reason for the constant distal curvature. During the fastest antennal movement in Fig. 3, angles between subsequent images of the antenna may exceed 15°, corresponding to movement velocities above 750° s^{-1}.

For quantitative investigation of antennal movement and its coordination with front legs, ten walks of four animals were analysed with a sampling interval of 40 ms, yielding a total of 43 s of detailed movement analysis (approx. 38 step cycles on each side). A single representative example is illustrated in Figs. 4A, 5A and 6 in order to simplify comparison between different stages of analysis.

The constant shape of the flagellum justifies the description of antennal movement pattern as the movement of the antennal tip, with the consequence that the curvature causes a systematic downward-shift of the calculated elevation by 8°. The typical antennal movement pattern is shown in Fig. 4A, where the spatial trajectories of the right and left antenna of a walking stick insect are plotted as polar coordinates in a sphere. Due to its rhythmicity, antennal movement can be described as a sequence of cycles. A typical movement cycle of an antenna involves a fast backward swing with an initial upward and a late downward component. This is followed by a slower forward movement, which is typically superimposed by a second up-and-down movement. Generally, the frequency of antennal elevation/depression cycles is about twice that of antennal abduction/adduction cycles. Analysis of video sequences with 200-Hz stroboscopic illumination revealed antennal ground contacts during downstrokes to occur in about 77% of cycles, indicating that they are no obligatory component of antennal movement in *C. morosus*.

In a resting position, i.e. during standing or thanatosis, the antennae of *C. morosus* point forwards, parallel to the body axis. Antennal movements away from this resting position may involve rotations around two joint axes. The location and orientation of these axes were determined in immobilised animals after fixing of one joint with glue, and imposing passive movement in the other joint (see Fig. 1B, H and text thereof). Figure 4B visualises the effect of rotation around these joint axes in a freely walking animal. If movement is restricted to the head-scape-joint, the antennal tip moves dorsolaterally from the resting position and back. Further movement towards the midline, or even crossing the midline, does not occur, probably because the head represents a mechanical boundary for ventro-medial movement. If movement is restricted to the scape-pedicel-joint, the antennal tip is moved dorso-medially and ventro-laterally, to about ±30° elevation with respect to the body axis. In this case, the antenna can reach the sagittal plane and even crosses it occasionally.

Because the experimental situation was to be kept as natural as possible, the insects were free to move their head during the recordings of antennal movement. As a consequence, the analysed trajectories contain a bias due to superimposed head movement. However, since antennal orientation was measured relative to the body long axis, i.e. the line from the antennal base to the hind coxae, head movement has a small impact. The maximum amplitude of the introduced 'head movement bias' was estimated from the width of the trajectory areas in Fig. 4B to be approximately 10–15° (judged from the width of the ellipse surrounding the trajectories). For comparison, the measured action range of the antenna was 80–90° wide.

Temporal co-ordination during walking

If antennal contacts were indeed to be used for quickly adapting to obstacles in the environment, one would expect that the observed antennal movement pattern was somehow spatially and temporally coordinated with the rhythmic stepping pattern of the legs.

There is strong coupling in the temporal coordination between antennae and front-legs, at least in case of the horizontal movement component of the antennae (Fig. 5). If the azimuth of the antennal tips and tibia-tarsus-joints relative to the body axis are plotted over time, the typical saw-toothed time-course of front-leg retraction/protraction is mirrored in a similar time course of antennal back-and-forth movement. However, the slow and fast phases of the saw-tooth pattern have opposite directions in antennae and front legs: whereas the slow movement component of leg movement is the retraction, the corresponding slow movement phase of the antennae is directed forward. Therefore, in terms of temporal features, the slow stance phase of a leg would be analogous to the slow forward movement of the ipsilateral antenna, whereas the fast swing movement of a leg would be analogous to the fast backward movement of the antenna.

Because the posterior extreme positions (PEP) of both leg movements and antennal movements are very distinct points in their time course (circles in Fig. 5A), they can be used to quantify the phase relationship between antennal and front leg movement. Plotting the phase lag of PEPs of antennae and left leg relative to the step cycle of the right leg reveals that antennal PEPs lead leg PEPs by 0.2–0.25 cycles (equivalent to 70–90°), and temporal coupling of antenna and front leg on one side of the animal matches that on the contralateral side (Fig. 5B). Furthermore, because the phase relationship between antennal movement cycle and front leg step cycle is similar to that between step cycles of neighbouring ipsilateral legs, the metachronous back-to-front wave of a standard textbook gait plot (e.g. Wilson 1966) can be extended to include the antennal movement cycle (Fig. 5C), bearing in mind that the movement direction is reversed for the antennae.

Spatial co-ordination of antennae and front legs

Temporal coupling of rhythmic leg and antennal movements of the same period, each of which having a rather stable spatial trajectory, implies considerable spatial coordination. Figure 6 visualises the extent of this spatial coordination by plotting the spatial trajectories of the antennal tips and the tibia-tarsus joints of the legs. Comparison of the side view of the two antennal trajectories in Fig. 6 (top) shows how densely the animal samples the antero-dorsal space during walking. Typically, up-down movements of both antennae are synchronous. Yet, the horizontal phase-shift causes alternating dorso-ventral loops in space. In the top view (Fig. 6, bottom) the lateral and medial extreme points of the antennal trajectories occur at rather fixed locations with respect to the leg trajectories. The antennal tip reaches its most lateral position close to the region where the next swing movement will take place, and its most medial position close to the midline, at a level of the current stance phase. The observation that the antennal tip typically is at the same level or ahead of the ipsilateral front leg is illustrated by the thin dashed lines, which connect coincident positions. The curvature of these lines always points at the direction of walking.

In order for a stick insect to use tactile information from the antennae for re-targeting or de-acceleration of an ongoing leg movement, antennal contact must lead leg contact. Knowing the spatio-temporal movement pattern of antennae and front legs allows to calculate the expected efficiency of antennal movements to detect a step of a certain height before tarsal contact. To do this, the lowest obstacle that would just be touched by an antenna but not by a leg was calculated for each instant in time in ten walking-sequences. The local minimum in

Fig. 5A–C Temporal co-ordination of antennae and legs. **A** Representative single traces of antennal abduction (*top diagram*) and tarsus retraction (*bottom diagram*), measured as the azimuth angle with respect to the body axis (0° = body axis). Alternating peaks indicate regular temporal coordination of the horizontal movement component in antennae and front legs. *Left and right limbs are plotted in dashed and solid lines*, respectively. *Solid circles labelled PEP* (posterior extreme position), mark two posterior extreme positions of the right front tarsus, which serve as a reference for the phase analysis shown in the juxtaposed diagram (**B**). *Open circles* mark the corresponding posterior extreme points in the remaining three traces. **B** Phase relationship of posterior extreme points in temporal measurements such as shown in **A**. Phase lead/lag of right (*r Ant*) and left antenna (*l Ant*) and left front leg (*l FL*) were measured with respect to the normalised step cycle of the right front leg, i.e. the period from one PEP to another. Absolute frequency of occurrence is plotted for 10 bins per normalised step cycle. Data from 10 walking-sequences from 4 animals, comprising 31 complete step cycles of right front legs. In five instances, the PEP of 'r Ant' occurred before the animal entered the field of view ($n = 26$, instead of $n = 31$). **C** Gait pattern of two non-consecutive walking episodes. *Black bars* mark retraction phases (stance phases) of the six legs (*l FL*, *l ML* and *l HL* for left front, middle and hind leg, respectively; analogously *r FL*, *r ML* and *r HL* for right legs). *Grey bars* mark protraction phases of antennae (*r Ant*: right, *l Ant*: left). Ticks mark 2-s intervals. *Dotted ellipses* group metachronous waves for both sides of the animal

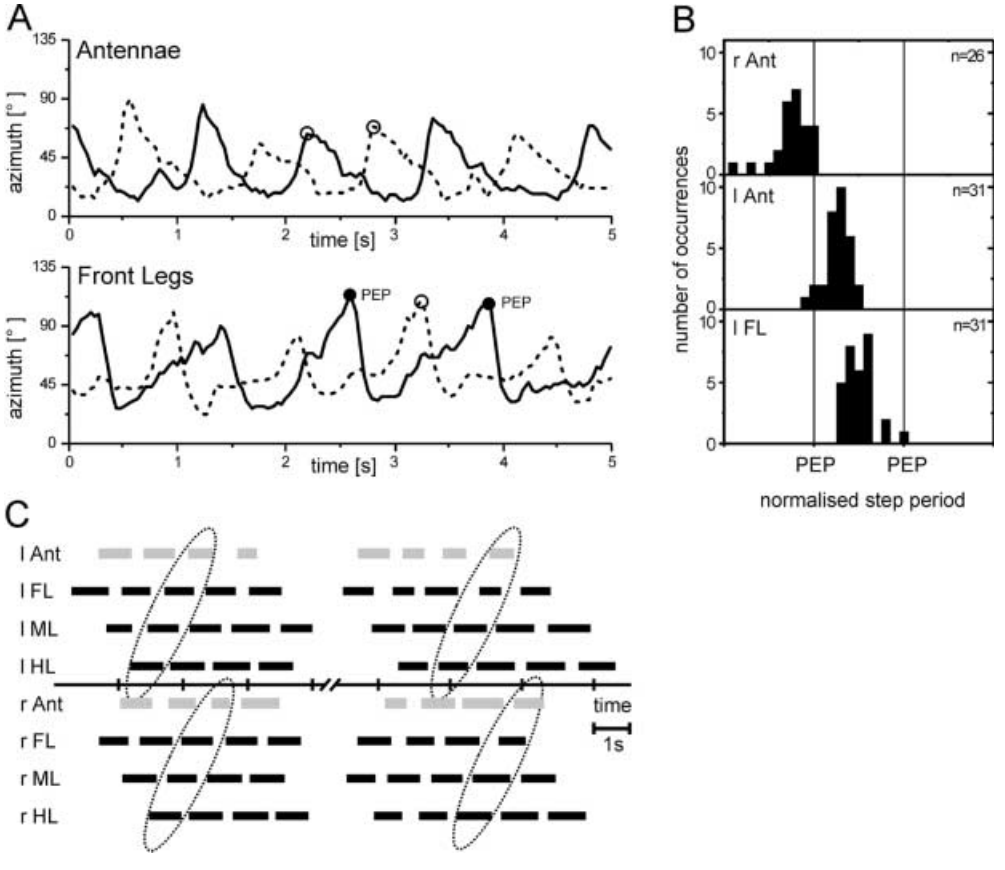

a sliding window of 400 ms width was then taken as an estimate of the lowest step that would be touched during about 15–20 mm movement progress in locomotion. The resulting curve indicates the expected frequency of an antenna to touch a 15- to 20-mm-wide rectangular obstacle of a given height before a tarsus gets there (Fig. 7). Because the antennae sometimes touch the ground, there is a chance to detect a step of height zero. The curve takes a sigmoidal course, crossing half maximum at an obstacle height of 6–7 mm. Above an obstacle height of 16 mm, the detection criterion is met in at least 90% of cases. This performance is achieved by an antennal movement pattern, in which the probability of the antennal tip being at a certain height is practically equal for all heights, resulting in a linear cumulative probability function (dotted line in Fig. 7).

Given this theoretical estimate, the performance of real walking stick insects was tested as they approached a 2-cm-wide step of a given height. Again, the results are plotted in Fig. 7, showing that the empirical frequency measures match the theoretical estimates quite well.

Discussion

Comparative anatomy of the antennal motor system

The antennal motor system of the stick insect *C. morosus* consists of three extrinsic tentorio-scapal muscles and two intrinsic scapo-pedicellar muscles. These muscles allow movement of the antennae around two hinge joint axes: one at the base of the scape and another at the base of the pedicel (Fig. 1B, H). The extrinsic muscles comprise two levator muscles and a composite, three-partite depressor muscle. The intrinsic muscles comprise one lateral and one medial muscle termed abductor and adductor, respectively (Fig. 1D, G, I). The antennal muscles are innervated by three nerves (N2–N4), only one of which (N3) is a pure motor nerve. N3 innervates both levator muscles. The remaining nerves N2 and N4 are mixed sensory-motor nerves, containing mechanoreceptive afferences as well as motor efferences. The depressor muscle is innervated by N4, the intrinsic muscles are innervated by both N2 and N4. The latter nerves form a cross-link (Fig. 2A, B).

The anatomy of antennal musculature of insects, and to a minor extent the anatomy of the antennal nerves, has been studied in many species and evolutionary trends have been discussed on various levels of systematic taxa (e.g. Imms 1939; Dudel 1977; Deshpande 1984). In this study we will restrict the anatomical comparison to four species in which the antennal motor system has been described at comparable detail: The locust *Locusta migratoria*, the cricket *Gryllus campestris*, the sphingid moth *Manduca sexta* and the honeybee, *Apis mellifera*.

In the cricket there are five extrinsic muscles, three levators and two depressors (muscles M4a-c and M5a-b, respectively, in Honegger et al. 1990). As in the stick insect, the depressors are innervated by a nerve that leaves the deutocerebrum separate from the other antennal nerves. The mesal depressor is additionally innervated by N3, which also innervates all levator muscles. In the cricket, N3 is a mixed sensory-motor nerve, as is N2. Both nerves branch off the main antennal nerve N1. Another similarity to the stick insect is a cross

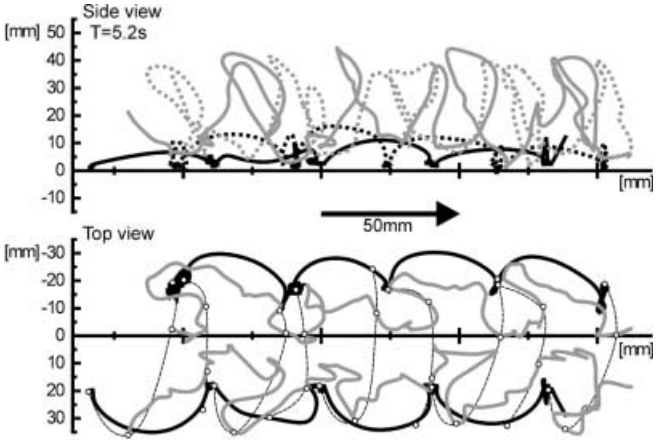

Fig. 6 Spatial co-ordination of antennae and front legs. Representative single trajectories of antennal tips (*grey lines*) and front leg tarsi (*black lines*) in external coordinates. *Top*: side view of an animal walking from left to right. *Solid lines* show trajectories of right limbs, *dotted lines* those of left limbs. *Bottom*: top view of same walk as above. All trajectories are B-spline interpolations of measured data points. *Open circles connected by thin dashed lines* show coincident positions in time (lines fitted by eye)

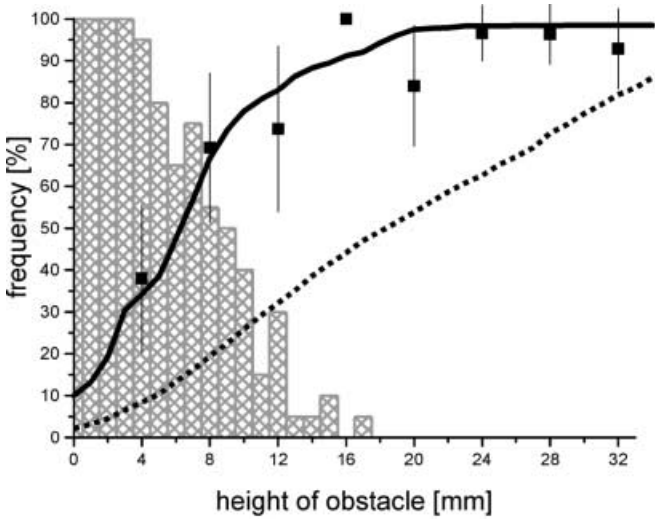

Fig. 7 Antennal movements predict touch probability of obstacles. *Solid black line* shows expected frequency of the event 'antennal contact leads leg contact' in dependence of obstacle height, given the known spatio-temporal movement pattern of antennae and front legs (see text for assumptions). *Filled squares* show empirical frequencies of same event in 208 walks of five animals (19–29 walks per height). Error bars denote 95% confidence intervals of binomial distribution. *Dotted line* shows cumulative probability of height of antennal tip, i.e. expected frequency of the tip being below the given height. *Cross-hatched columns* show simulation results of Cruse et al. (1998) for success rate of a stick insect model to climb a step of a given height (see Discussion)

link between N2 and N4. The situation of the two intrinsic muscles and their innervating nerves N2 and N4, *G. campestris* and *C. morosus* are virtually identical.

In the locust, Gewecke (1972) described only two extrinsic muscles, one depressor and one levator, whereas Imms (1939, his Fig. 1) illustrated the extrinsic musculature of *L. migratoria* with two levator parts and two depressor parts, suggesting that there are two distinct proximal insertion sites for both muscles. According to Gewecke, both extrinsic muscles are innervated by a nerve which, like the N4 in crickets and stick insects, leaves the deutocerebrum separately from the main antennal nerve, however, together with an additional sensory nerve innervating hair fields on the head. This nerve later separates into a depressor nerve and a levator nerve, which may be homologous to the N3/N4 situation in crickets and stick insects. The locust nerve innervating the two intrinsic muscles (three drawn by Imms), branches off the lateral N1 and later splits into an adductor branch and an abductor branch. Given the fact that the phylogenetic relationship between crickets and locusts is closer than either of their relationship to the stick insect, it can be argued that the innervation of the antennal motor system of the stick insect is close to the 'bauplan' of the common ancestor of all Orthoptera and Phasmatodea. Following this interpretation, the locust antennal motor system would have to be considered as more reduced and derived, possibly reflected in the short antennae of the taxon Caelifera (incl. *L. migratoria*), which no longer allows tactile employment to the same extent as it is possible with the long antennae of the taxon Ensifera (incl. *G. campestris*) and the taxon Phasmatodea (incl. *C. morosus*).

Compared to the three mentioned hemimetabolous species, the antennal motor system of the holometabolous species *M. sexta* (Kloppenburg et al. 1997) and *A. mellifera* (Snodgrass 1956; Kloppenburg 1995) are rather different, particularly with respect to the head-scape joint and the corresponding muscles. In this joint, bees and moths have a single condylus, the so-called antennifer, allowing at least two degrees of freedom of rotation (pitch and yaw). Accordingly, the five extrinsic muscles of *M. sexta* and the four extrinsic muscles of *A. mellifera* not only form a levator/depressor system (although they are named like that by Kloppenburg et al.) but also form an abductor/adductor system. Theoretically, even rotations around the long axis of the scape are possible here, although probably only of small amplitudes. Concerning the intrinsic muscles, *M. sexta* has an additional third muscle to the two that would suffice to rotate the pedicel around a hinge joint. The situation of the intrinsic musculature in the bee is similar to that in the locust.

Antennal motoneurons

In the stick insect, there are at least 14, probably 17 motoneurons involved in the motor control of antennal movement. This includes 5 levator, 4–5 depressor, 3 adductor and 2–4 abductor motoneurons and one CI neuron (Fig. 2C–F). Because the cobalt stains did not reliably and clearly fill the fine dendrites for all motoneurons, dendritic arborisations were not traced but only delineated in their entirety for each functional group. These 'dendrite areas' show a conspicuous circular dendrite-free region in levator and abductor motoneurons (Fig. 2C, F). The lack of this dendrite-free region in depressor and adductor motoneurons may indicate their arborisation at a different depth in the neuropile. The motoneuron somata cluster in three regions in the periphery of the AMMC (Table 1). The lateral soma region contains most neurons, the posterior region contains only two twin pairs and the anterior region contains 1 levator, 1 depressor and possibly 1 abductor motoneuron. In the cricket, 18 antennal motoneurons have been described (Honegger et al. 1990) and in the locust there are 19 (Bauer and Gewecke 1991), leaving them with one or two neurons more to control antennal movement compared to the stick insect. Although the different brain shapes of crickets and stick insects make it difficult to label homologous neurons, it is interesting to note that the numbers of motoneurons in each functional group in *G. campestris* is similar to *C. morosus*. The cricket has one levator and one depressor motoneuron twin pair, plus an adductor twin pair which does not occur in the stick insect. *A. mellifera* (Kloppenburg 1995) and *M. sexta* (Kloppenburg et al. 1997) have 15 and 12 motoneurons, respectively, leaving them with fewer motoneurons to control more degrees of freedom than the stick insect, cricket and locust.

The CI of the stick insect antenna was identified only anatomically by its innervation of all muscles (Rathmayer and Bevengut 1986). A CI has been shown to exist in the antennal motor system of the cricket *G. bimaculatus* (Allgäuer and Honegger 1993) and the crayfish *Euastacus armatus* (Sandeman and Wilkens 1983), as well as in the leg motor system of various arthropods (e.g. Pearson and Bergman 1969).

The midline location of three protocerebral somata that were found in some backfills of the nerve N2 is reminiscent of the sensory neurons of a stretch receptor described by Bräunig (1985) for the locust *Schistocerca gregaria*. Bräunig also refers to unpublished observation of a homologous antennal stretch receptor in the cricket. So far, no such stretch receptor has been found in the stick insect. The identity of these neurons therefore remains unclear.

Finally, Bräunig et al. (1990) and Honegger et al. (1990) reported the existence of dorsal unpaired median neurons in the suboesophageal ganglion of crickets and locusts which also innervate antennal muscles. In the nerve backfills in *C. morosus*, no neurites were found to descend through the circum-oesophageal connectives.

Functional anatomy and typical movement pattern

The resting position of the antennae is close to the ventro-medial extreme position. Depression of the scape

does not move the antenna much below the horizon and never across the sagittal plane (Fig. 4B). During walking, *C. morosus* moves its antennae in a characteristic cyclic pattern. Each movement cycle comprises a fast backward movement and a slower forward movement, superimposed by two up-down movements (Figs. 4, 5). This pattern is caused by rotations around two joint axes (Fig. 1B, H). Since these axes are neither orthogonal to each other nor aligned with respect to the horizontal or vertical body axis, the standard terminology, i.e. depressor/levator and adductor/abductor, is somewhat misleading. In reality, pure horizontal movement would require co-contractions of the levator and abductor or, for the opposite direction, of depressor and adductor. Analogously, pure up-down movement also requires appropriate co-contractions. The standard muscle terminology is justified by the close phylogenetic relationship between *C. morosus* and the cricket (see above). In crickets, as well as in locusts, the head-scape-joint axis is more ore less aligned with the horizontal plane and the scape-pedicel-joint axis is aligned with the vertical body axis (Gewecke 1972; Honegger et al. 1990). Compared to this orthogonal construction, the situation in the stick insect is rotated outwards. One possible functional reason for this peculiar alignment of joint axes might be that it reduces required energy for the execution of the observed typical antennal movement pattern. Another advantage of slanted joint axes might be to increase both positioning-accuracy and sensory resolution along the dividing line between the two joint axes. The underlying idea is as follows: given that rotation around each one of two joint axes is independent of the other, and angular precision of both antagonistic muscle systems is limited, this precision will be improved during combined action by the cosine of half the dividing angle between the two movement directions (Fig. 8). Accordingly, in the case of non-orthogonal axes, precision will be better along the axis set by the wider angle. An analogous argument applies for sensory resolution of joint proprioceptors. According to the antennal movement directions defined by the joint axes in the stick insect (Fig. 4B) maximum precision would be expected for dorso-lateral movements.

Antennal movement in the stick insect may reach velocities above 750° s^{-1}. Judging from spontaneous antennal movements in walking crickets (Horseman et al. 1998), they can reach similarly high velocities. In comparison, antennal retraction in some ant species can reach velocities of several thousand degrees per second (Ehmer and Gronenberg 1997), but this retraction behaviour is likely to be a specialised ballistic movement rather than a continuously controlled movement.

Spatio-temporal co-ordination of antennae and legs, and the tactile use of antennae as 'mechanical probes'

Analogous to the leg movement cycle, the antennal movement can be functionally divided into two phases: a fast backward directed movement phase, and a slow forward movement phase (Fig. 5). These phases correspond to swing and stance phases of the leg step cycle, yet the movement direction of the antennal cycle is opposed to that of the leg cycle during forward walking. Crickets show spontaneous rhythmic antennal movement during walking (Horseman et al. 1997) however coupling with leg movements is only loose. As it is during the forward sweeps that the stick insect antennae sample previously un-probed space (Fig. 6), functionally this cycle phase can be called a 'search phase'. A search devoid of any contacts can signal 'free space' to the ipsilateral front leg, whereas a contact during the search phase could trigger re-targeting of the next swing movement of a front leg. Fast re-targeting movements of front legs are frequently observed in walking stick insects, and a detailed description of these movements in their relation to preceding antennal contacts is currently in progress (V. Dürr, unpublished observations). Direct evidence for use of tactile cues to the antennae during locomotion comes from work on potato beetles, which incline their body axis upon tactile contacts with obstacles (Pelletier and McLeod 1994).

If the stick insect antennae were to be used as mechanical probes and their movement was to aid tactile localisation of obstacles, appropriate spatio-temporal coordination of antennal and leg movements would be a requirement for efficient obstacle detection. Here, efficiency is thought of as the ability to exploit antennal contacts for immediate alteration of the on-going locomotor program. Antennal movements of *C. morosus* were shown to be tightly coupled to leg movements in time (Fig. 5) and space (Fig. 6) and spatial trajectories of antennae and legs were used to predict the probability to touch an obstacle first with the antennae (Fig. 7). This

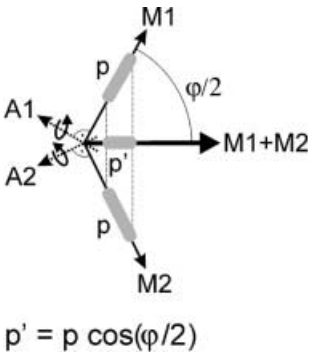

Fig. 8 Improvement of positioning precision by two joint axes. Independent rotation of an antenna around two the joint axes A1 and A2 (see Fig. 1H) would lead to motion of the antennal tip along the *arrows M1 and M2*, respectively, which represent the projections of the antennal tip on the drawing plane. Combined rotation would move the projection of the tip along M1 + M2. If positioning of the tip along M1 and M2 was limited by precision *p*, their combined effort would improve positioning along M1 + M2 by the cosine of $\varphi/2$, if positioning error along M1 and M2 were independent of each other. φ is the angle enclosed by M1 and M2, equivalent to an angle between A1 and A2 (in this case the larger angle)

theoretical prediction was confirmed by empirical data, showing that the typical antennal movement pattern alone is sufficient to explain the behavioural performance. As a blind stick insect also displays the typical movement pattern vision is probably not used in obstacle detection (V. Dürr, unpublished observations). Certainly, vision does not improve performance. Interestingly, the 50% chance to detect an obstacle first with the antennae is reached at an obstacle height of 6–7 mm, which is approximately equal to half the 'clearance' of the animal, i.e. the height of the prothorax. From computer simulations of Cruse et al. (1998) it is known, that an artificial neural network controller of hexapod walking (WalkNet) can overcome obstacles without possessing antennae. The results of Cruse et al. are added into Fig. 5 as the frequency of WalkNet to successfully climb a step of a given height. The criterion for 'success' allowed instabilities shorter than one average swing phase. WalkNet performs well up to obstacle heights of 5–8 mm, but there are problems with higher obstacles. This could be avoided if it had mechanical probes with the properties of stick insect antennae, because at critical obstacle heights these antennae could transfer early information about the forthcoming obstacle and elicit adaptation to the new circumstances in time. Of course, this is no proof of antennal tactile function. However, because WalkNet uses the geometry of the stick insect and contains a lot of the present knowledge of biological hexapod walking, it is certainly indicative of antennal tactile usefulness.

Acknowledgements We are grateful to T. Authmann, A. Exter, S. Matzak and D. von Trotha for technical assistance, and to M. Gebhardt and H. Cruse for valuable comments on earlier versions of the manuscript. This work was supported by grant CR 58/9-2 of the Deutsche Forschungsgemeinschaft, DFG.

References

Allgäuer C, Honegger H-W (1993) The antennal motor system of crickets: modulation of muscle contractions by a common inhibitor, DUM neurons, and proctolin. J Comp Physiol A 173:485–494

Altman JS, Tyrer NM (1980) Filling selected neurons with cobalt through cut axons. In: Strausfeld NJ, Miller TA (eds) Neuroanatomical techniques. Insect nervous system. Springer, Berlin Heidelberg New York, pp 373–402

Bässler U (1983) Neural basis of elementary behavior in stick insects. Springer, Berlin Heidelberg New York

Bauer C, Gewecke M (1991) Motoneuronal control of antennal muscles in *Locusta migratoria*. J Insect Physiol 37:551–562

Bräunig P (1985) Mechanoreceptive neurons in an insect brain. J Comp Neurol 236:234–240

Bräunig P, Allgäuer C, Honegger HW (1990) Suboesophageal DUM neurons are part of the antennal motor system of locusts and crickets. Experientia 46:259–261

Cappe de Baillon P (1936) L'organe antennaire des Phasmes. Bull Biol France Belg 70:1–35

Cruse H (1990) What mechanisms coordinate leg movement in walking arthropods? TINS 13:15–21

Cruse H, Kindermann T, Schumm M, Dean J, Schmitz J (1998) Walknet – a biologically inspired network to control six-legged walking. Neural Networks 11:1435–1447

Deshpande SB (1984) Studies on the morphological evolutionary trends of antennary muscular patterns in insects. J Anim Morphol Physiol 31:53–66

Dudel H (1977) Vergleichende funktionsanatomische Untersuchungen über die Antennen von Dipteren. I. Bibliomorha, Homoeodactyla, Asilomorpha. Zool Jahrb Anat 98:203–308

Dürr V (1999) Spatial searching strategies of the stick insect, using antennae and front legs (abstract). Proc Göttingen Neurobiol Conf 27:212

Ehmer B, Gronenberg W (1997) Antennal muscles and fast antennal movements in ants. J Comp Physiol B 167:187–296

Erber J, Pribbenow B, Grandy K, Kierzek S (1997) Tactile motor learning in the antennal system of the honeybee (*Apis mellifera* L.). J Comp Physiol A 181:355–365

Erber J, Kierzek S, Grandy K (1998) Tactile learning in the honeybee. J Comp Physiol A 183:737–744

Field LH, Matheson T (1998) Chordotonal organs of insects. Adv Insect Physiol 27:1–288

Gewecke M (1972) Bewegungsmechanismus und Gelenkrezeptoren der Antennen von *Locusta migratoria*. Z Morphol Tiere 71:128–149

Hansson BS (1999) Insect olfaction. Springer, Berlin Heidelberg New York

Homberg U, Christensen TA, Hildebrand JG (1989) Structure and function of the deutocerebrum in insects. Annu Rev Entomol 34:477–501

Honegger H-W, Allgäuer C, Klepsch U, Welker J (1990) Morphology of antennal motoneurons in the brains of two crickets, *Gryllus bimaculatus* and *Gryllus campestris*. J Comp Neurol 291:256–268

Horseman BG, Gebhardt MJ, Honegger H-W (1997) Involvement of the suboesophageal and thoracic ganglia in the control of antennal movements in crickets. J Comp Physiol A 181:195–204

Hoy RR, Popper AN, Fay RR (1998) Comparative hearing: insects. Springer, Berlin Heidelberg New York

Imms AD (1939) On the antennal musculature in insects and other arthropods. Q J Microsc Sci 81:273–320

Kevan PG, Lane MA (1985) Flower petal microtexture is a tactile cue for bees. Proc Natl Acad Sci USA 82:4750–4752

Kittmann R, König Y (1995) The antennal motor system of the stick insect (abstract). Proc Göttingen Neurobiol Conf 23/II:216

Kloppenburg P (1995) Anatomy of the antennal motoneurons in the brain of the honeybee (*Apis mellifera*). J Comp Neurol 363:333–343

Kloppenburg P, Camazine SM, Sun XJ, Randolph P, Hildebrand JG (1997) Organization of the antennal motor system in the sphinx moth *Manduca sexta*. Cell Tissue Res 287:425–433

Mill PJ (1976) Structure and function of proprioceptors in the invertebrates. Chapman and Hall, London

Obermayer M, Strausfeld NJ (1980) Silver-staining cobalt sulfide deposits within neurons of intact ganglia. In: Strausfeld NJ, Miller TA (eds) Neuroanatomical techniques. insect nervous system. Springer, Berlin Heidelberg New York, pp 403–427

Pearson KG, Bergman SJ (1969) Common inhibitory motoneurones in insects. J Exp Biol 50:445–471

Pelletier Y, McLeod CD (1994) Obstacle perception by insect antennae during terrestrial locomotion. Physiol Entomol 19: 360–362

Quicke DLJ, Brace RC (1979) Differential staining of cobalt- and nickel-filled neurones using rubeanic acid. J Microsc 115:161–163

Rathmayer W, Bevengut M (1986) The common inhibitory neuron innervates every leg muscle in crabs. J Comp Physiol A 158:665–668

Romeis B (1989) Mikroskopische Technik. Urban und Schwarzenberg, München Wien Baltimore

Rospars JP (1988) Structure and function of the insect antennodeutocerebral system. Int J Insect Morphol Embryol 17:243–294

Sandeman DC, Wilkens L (1983) Motor control of movements of the antennal flagellum in the Australian crayfish, *Euastacus armatus*. J Exp Biol 105:253–273

Schneider P, Reitberger K (1988) Beinkoordination und Lauf über Hindernisse von *Carabus violaceus* (Coleoptera). Zool Jahrb Physiol 92:351–364

Slifer EH (1966) Sense organs on the antennal flagellum of a walkingstick *Carausius morosus* Brünner (Phasmida). J Morphol 120:189–202

Snodgrass RE (1956) Anatomy of the honey bee. Cornell University Press, Ithaka

Stavenga DG, Hardie RC (eds) (1989) Facets of vision. Springer, Berlin Heidelberg New York

Strausfeld NJ, Miller TA (eds) (1980) Neuroanatomical techniques. Insect nervous system. Springer, Berlin Heidelberg New York

Weide W (1960) Einige Bemerkungen über die antennalen Sensillen sowie über das Fühlerwachstum der Stabheuschrecke *Carausius (Dixippus) morosus* Br. (Insecta: Phasmida). Wiss Z Martin-Luther-Univ Halle-Wittenberg Math-Naturwiss Reihe IX/2:247–250

Weidler DJ, Diecke FPJ (1969) The role of cations in conduction in the central nervous system of the herbivorous insect *Carausius morosus*. Z Vergl Physiol 196:372–399

Wilson DM (1966) Insect walking. Annu Rev Entomol 11:103–122

Yack JE (1993) Janus green B as a rapid, vital stain for peripheral nerves and chordotonal organs in insects. J Neurosci Methods 49:17–22